Ball-type supramolecular metallophthalocyanines with eight perfluorodecyl units: chemosensors for SO_2 and electrocatalysts for oxygen reduction

Metin Özer,[a] Ahmet Altındal,[b] Ali Rıza Özkaya[a] and Özer Bekaroğlu*[c]

Received 20th October 2008, Accepted 8th December 2008
First published as an Advance Article on the web 11th February 2009
DOI: 10.1039/b818455k

Heptadecafluorodecyl-substituted cofacial or ball-type bis-metallophthalocyanines (BTMPcs) have been prepared. The redox properties of the complexes and their catalytic activities for oxygen reduction were studied. The occurrence of stepwise one-electron redox processes during the voltammetric measurements in solution suggested the formation of stable mixed-valence species of the complexes, as a result of the intramolecular interactions between two cofacial Pc units. The ball-type Co(II) complex displayed excellent catalytic activity for oxygen reduction which is probably due to the rigid cofacial structure involving two redox-active metal centers, which are capable of binding O_2. dc and ac conduction properties of BTMPcs [M = Co(II) **3** and Cu(II) **4**]thin films have been investigated in the frequency range of 40 to 10^5 Hz and temperature 290–440 K. The dc results showed an activated conductivity dependence on temperature for all films. The analysis of the obtained data showed that the correlated barrier hopping (CBH) model is the dominant conduction mechanism for electron transport in the films. The gas sensing properties of the films for SO_2 were also investigated over the same temperature range. Although a very high response to SO_2 gas has been obtained for the film of **3** at room temperature, the film of **4** was not sensitive to the same gases.

1. Introduction

Cofacial or ball-type metallophthalocyanines (BTMPcs) are a new type of compound which appeared in the literature for the first time a few years ago.[1] It was followed by several novel BTMPcs bridged with different substituents such as *tert*-butylcalix[4]arene,[2] 1,1′-methylenedinaphthalen-2-ol,[3] pentaerythritol[4] and its crown ether derivative,[5] 1a,8b-dihydronaphtho[*b*]naphthofuro[3,2-*d*]-furan-7,10-diol,[6,7] 4,4′-isopropylidendioxydiphenol,[8] and phenolphthalein.[9] The spectroscopic, optical, electrical, electrochemical and gas sensing properties of these BTMPcs have been studied by our group to understand their characteristics.[2–9] Our studies showed that these properties are considerably different from their parent monomer.

MPcs with multiple electron-withdrawing peripheral substituents are more stable and more active products for their applications as compared to unsubstituted MPcs. Moreover, the electron-withdrawing substituents at the periphery of Pc cause a large increase in the ionization potential (IP), and thus in the chemical and thermal strength of the system.[10] Although a large number of fluorinated Pc complexes have been synthesized and characterized, BTMPcs with vicinally perfluorinated alkyl groups have not been studied to the best of our knowledge. Our continuing efforts on the combination of cross-linked BTMPcs with *aliphatic* perfluorinated alkyl substituents have enabled us to accomplish products with improved physical properties. The present paper describes the synthesis of BTMPcs containing eight heptadecafluorodecyl groups. First, precursor cofacial dimers of BTMPcs [Co(II) **1** and Cu(II) **2**] were prepared and characterized by the reported method.[4] Next, the novel heptadecafluorodecyl substituted BTMPcs [Co(II) **3** and Cu(II) **4**] were prepared by their condensation reaction. The electrochemical, electrocatalytic, electrical and SO_2 sensing characteristics of **3** and **4** were also studied and discussed.

2. Results and discussion

The synthesis of heptadecafluorodecyl substituted BTMPcs (**3** and **4**) has been achieved by the nucleophilic substitution of precursor cofacial dimers of BTMPcs (**1** and **2**) bearing eight hydroxy groups on the four pentaerythritol moieties with heptadecafluoro-10-iododecane (HDFID) (Scheme 1). The substitution reaction was carried out in DMF at 120 °C in the presence of sodium hydride (NaH) as base. Although complex **3** was separated on a silica gel packed column using a THF–DMF system (5–50%), compound **4** was purified successively by precipitating the dissolved complex **4** in hot acetic acid, water, methanol and acetone due to the limited solubility of **4** in polar aprotic solvents such as DMF and DMSO. The structures of the isolated complexes **3** and **4** were confirmed by elemental analysis, FT-IR, UV-vis and MALDI-TOF-mass spectroscopy.

The FT-IR spectra of **3** and **4** indicated typical aliphatic-CH vibrational bands at 2937–2880 cm^{-1} and at 2925–2853 cm^{-1}, which were assigned to the erythritol C–H of the Pc assemblies. The broad vibrational OH band seen at about 3402 cm^{-1} in the precursors was not present in the FT-IR spectra of **3**

[a]*Department of Chemistry, Marmara University, 34722, Göztepe-Istanbul, Turkey. E-mail: metinozer@marmara.edu.tr; aliozkaya@marmara.edu.tr; Fax: +90 216 3478783; Tel: +90 216 3479641*
[b]*Department of Physics, Marmara University, 34722, Göztepe-Istanbul, Turkey. E-mail: aaltindal@marmara.edu.tr; Fax: +90 216 3478783; Tel: +90 216 3479641*
[c]*Department of Chemistry, Technical University of Istanbul 34469, Maslak-Istanbul, Turkey. E-mail: obek@itu.edu.tr; Fax: +90 216 3860824; Tel: +90 216 3479641*

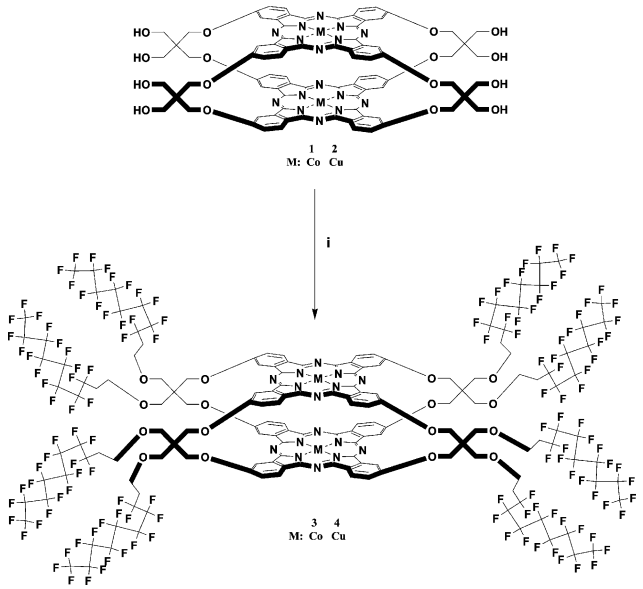

Scheme 1 (i) NaH and HDFID in DMF at 120 °C.

and **4**. Additionally the characteristic C–F bands of **3** and **4** appeared at 1230–1120, 1226–1116 cm^{-1}, respectively. The UV-vis measurement of **3** and **4** in DMF (4.3×10^{-5} and 2.7×10^{-5} mol L^{-1} respectively) showed spectra characteristic of these macrocyclic compounds. The spectra present strong B and Q bands that have been assigned to $\pi \rightarrow \pi^*$ transitions. The Q bands of the complexes are observed at around 675 nm. The UV-vis spectra of **3** and **4** are shown in Fig. 1.

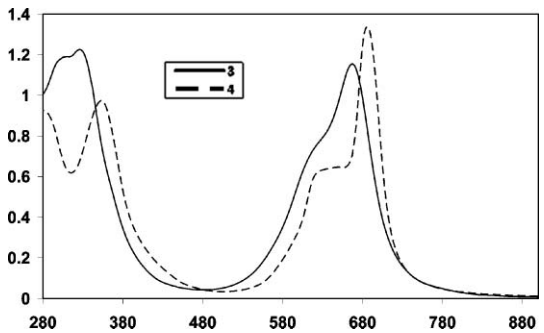

Fig. 1 UV-vis spectrum of heptadecafluorodecyl subtituted BTMPc derivatives **3** and **4** in DMF.

Heptadecafluorodecyl substituted **3** and **4** complexes were analyzed by MALDI-MS. Many different MALDI matrices were tested to obtain highly resolved spectra. The best matrices for **3** and **4** were found to be 2,5-dihydroxybenzoic acid (DHB) and α-cyano-4-hydroxycinnamic acid (CHCA) respectively. Highly resolved MALDI mass spectra could not be obtained for both complexes because of the short life time of the protonated molecular ions. In other words, the stability of the protonated ion form of the complexes in the gas phase under MALDI-MS conditions was low. In the MALDI-MS spectrum of complex **3**, besides the protonated molecular ion peak, three fragment peaks were observed between 1000 and 2600 Da (highest mass was at 2535 corresponding to one part of the complex having a phthalocyanine core with cobalt and two side chains with florine rich functional group) (Fig 2). These types of fragment ion were due to the loss of the side chains

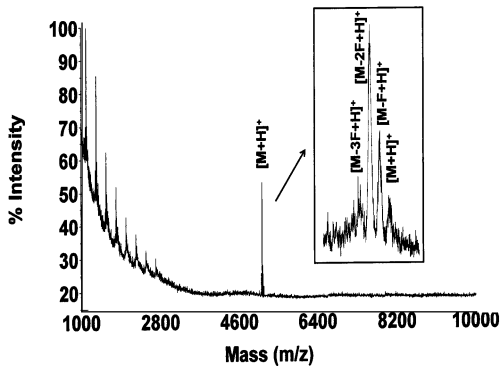

Fig. 2 Positive ion and linear mode MALDI-MS spectrum of supramolecular cobalt complex **3** in 2,5-dihydroxybenzoic acid MALDI matrix using a nitrogen laser accumulating 50 laser shots. Inset spectrum shows expanded protonated molecular ion region.

containing a high number of fluorine containing groups after symmetrical decomposition of the complexes. The mass difference between the fragment peak groups was about 433 Da and the mass difference in each main fragment peak was 19 Da which corresponds to fluorine elimination from the main fragment ions containing $C_9H_2F_{17}$ functional groups. This difference indicates the existence of fluorine in the complex molecules.

In the case of copper complex **4**, beside the protonated molecular ion peak of the complex, some intense signals representing the fragment ions in the mass range between 600 and 2200 Da were observed (highest mass of the fragment ion was found to be 2092 Da corresponding to one part of the complex having one phthalocyanine core with copper and one side chain with fluorine rich functional groups). These fragment ions showed that some different side chain fragmentations occurred readily from the complex molecule under the laser shots. The evaluation of these peak masses showed that these ions were due to the fragmentation of the complex (Fig 3).

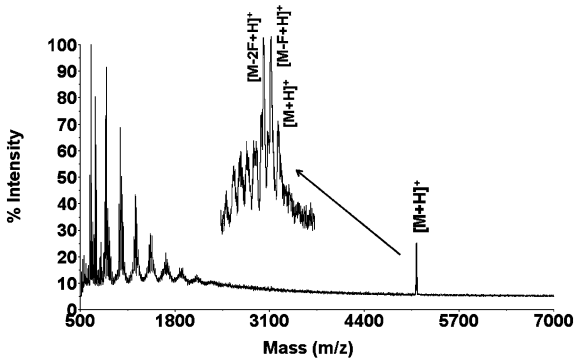

Fig. 3 Positive ion and reflectron mode MALDI-MS spectrum of supramolecular Cu complex **4** in α-cyano-4-hydroxycinnamic acid (CHCA) (20 mg mL^{-1} in tetrahyrofuran with 0.5% trifluoroacetic acid) MALDI matrix using nitrogen laser accumulating 50 laser shots. Inset spectrum shows expanded molecular mass region of the complex.

The electrochemical properties of the complexes were examined by cyclic voltammetry and controlled-potential coulometry in DMSO–TBAP (tetrabutylammonium perchlorate). Voltammetric data for the complexes are presented in Table 1, and a typical cyclic voltammogram of **3** is shown in Fig. 4. Each BTMPc

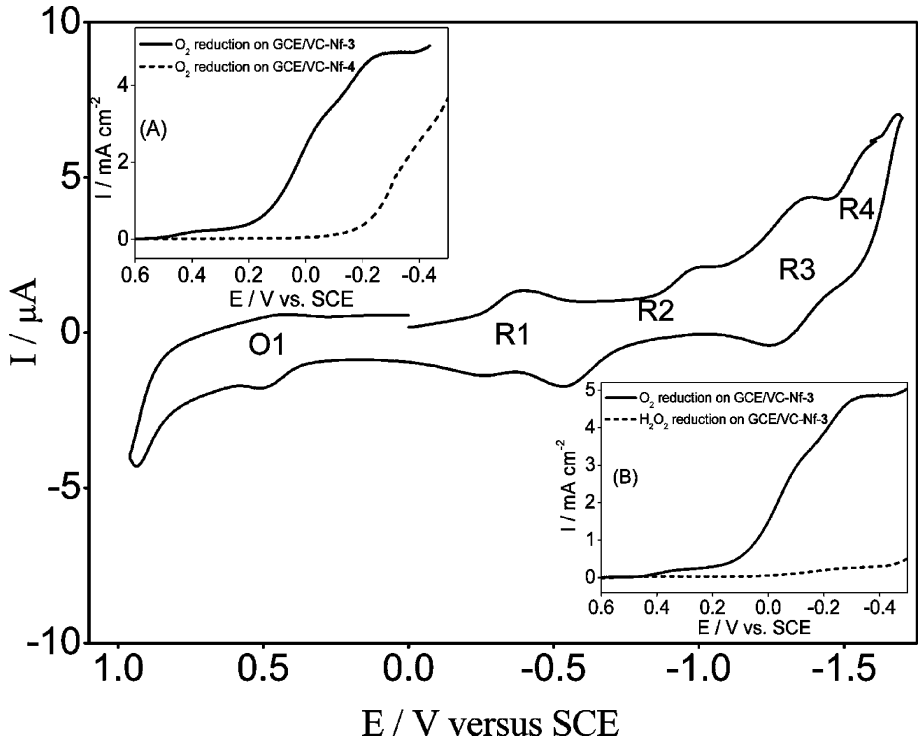

Fig. 4 Cyclic voltammogram of **3** (2.00×10^{-4} M) at 0.050 V s^{-1} on Pt in DMSO–TBAP solution. Inset A: Linear sweep voltammograms at 0.005 V s^{-1} on rotating (2500 rpm) GCE/VC-Nf electrodes adsorbed with **3** or **4** in O_2 saturated 0.5 M H_2SO_4 aqueous solution. Inset B: Linear sweep voltammograms at 0.005 V s^{-1} on rotating (2500 rpm) GCE/VC-Nf-**3** electrodes in 0.5 M H_2SO_4 aqueous solution, O_2 saturated or containing 1 mM H_2O_2 in the absence of O_2.

Table 1 Voltammetric data for **3** and **4** on Pt in DMSO–TBAP

Complex	Redox process[a]	$E_{1/2}$[b]/V (*vs.* SCE)	ΔE_p[c]/V	I_{pa}/I_{pc}[d]	$\Delta E_{1/2}$[e]/V
Co_2Pc_2 **3**	O1	0.47	0.13	$I_{pa} >> I_{pc}$[f]	0.80
	R1	–0.33	0.13	0.95	
	R2	–0.76	0.53[f]	0.62[f]	
	R3	–1.30	0.12	0.98	
	R4	–1.55	0.07	$I_{pc} \approx I_{pa}$	
Cu_2Pc_2 **4**	O1	0.29	0.15	0.92	0.86
	R1	–0.57	0.08	1.00	
	R2	–0.99	0.10	0.96	

[a] For all redox processes, the number of electrons transferred per molecule was found to be one from controlled-potential coulometric measurements. [b] $E_{1/2}$ values were measured by cyclic voltammetry [$E_{1/2} = (E_{pa} + E_{pc})/2$]. [c] $\Delta E_p = E_{pa} - E_{pc}$ at 0.050 V s^{-1}. [d] I_{pa}/I_{pc} for reduction, I_{pc}/I_{pa} for oxidation processes at 0.050 V s^{-1} scan rate. [e] $\Delta E_{1/2} = E_{1/2}$ (first oxidation) – $E_{1/2}$ (first reduction). [f] The peak current ratio deviates considerably from unity for the O1 and R2 couples of **3**. Also, the ΔE_p value is very high for the R2 couple of **3**. Electron transfer reactions for these couples should be associated by some chemical reaction.

complex involving two cofacial Pc rings displayed stepwise one-electron reduction and oxidation processes, usually indicating the formation of stable mixed-valence reduced and oxidized species. The redox processes of various BTMPc complexes associated with the formation of various mixed-valence species were identified previously by our group.[2–4,6,8,9] These studies suggested that the first two reduction and two oxidation processes in ball-type or cofacial Co_2Pc_2 complexes are metal-based in polar coordinating solvents such as DMSO and DMF while the others are Pc-ring based. Since compound **3** is a binuclear cofacial complex involving two Co(II) centers, the oxidation and the first two reductions correspond to $[Co^{II}Pc(-2).Co^{III}Pc(-2)]^+$/$[Co^{II}Pc(-2)]_2$,$[Co^{II}Pc(-2)]_2$/$[Co^{II}Pc(-2).Co^{I}Pc(-2)]^-$ and $[Co^{II}Pc(-2).Co^{I}Pc(-2)]^-$/$[Co^{I}Pc(-2)]_2^{2-}$ redox processes, respectively. On the other hand, the third and fourth reductions should be related to the splitting of the Pc(–2)/Pc(–3) couple, and thus ligand-based, corresponding to $[Co^{I}Pc(-2)]_2^{2-}$/$[Co^{I}Pc(-2).Co^{I}Pc(-3)]^{3-}$ and $[Co^{I}Pc(-2).Co^{I}Pc(-3)]^{3-}$/$[Co^{I}Pc(-3)]_2^{4-}$ redox processes, respectively. On the other hand, since the Cu(II) metal center is redox-inactive in Pc complexes, all the redox processes of **4** are ring-based. The separation between the half-peak potentials of the first reduction and the first oxidation for each BTMPc complex ($\Delta E_{1/2}$) was remarkably low (0.80 V for **3** and 0.86 V for **4**) as compared with those of mono Pcs which is in the range 1.30–1.80 V. Such voltammetric behavior results from strong intermolecular interactions between the two Pc rings and/or metal centers linked cofacially at two sides with four arms, and consistent with the rigid structure of BTMPcs.

To the best of our knowledge, there have not been any reports on the electrocatalytic activity of BTMPcs towards oxygen reduction (OR), although it was reported that the catalytic activity of porphyrins towards OR is enhanced by a cofacial structure.[11,12] Inset A in Fig. 4 shows linear sweep voltammograms (LSVs) recorded on a rotating (2500 rotations per minute) **3** or **4** modified glassy carbon disk electrode (GCE) supported by active carbon, Vulcan XC-72 (VC) and Nafion® (Nf) in O_2 saturated 0.5 M H_2SO_4 aqueous solution. OR occurs at much more positive

potentials at the VC-Nf-**3** modified GCE than those at the VC-Nf-**4** modified one, clearly indicating the higher catalytic activity of the former. The maximum current density at the diffusion plateau for **3** is approximately 5.0 mA cm^{-2} (inset A in Fig. 4). This value is comparable to the limiting current densities obtained previously with Pt/C, polyaniline/FePc and FePc/C electrodes,[13] and implies that OR at VC-Nf-**3** modified GCE occurs *via* a 4-electron process with water as the main product. Because H_2O_2 is an intermediate product of OR, investigating its reduction can help in understanding the reaction mechanism. Inset B in Fig. 4 displays LSV recorded in 0.5 M H_2SO_4 containing 1 mM H_2O_2 in the absence of O_2, together with the polarization curve of OR. Comparing LSVs of O_2 and H_2O_2 in the absence of O_2, it is concluded that the CoPc (**3**) modified electrode does not catalyze H_2O_2 reduction in the lower overpotential region of the OR polarization curve. In addition, it shows a very poor catalytic activity towards H_2O_2 reduction in the higher overpotential region of the OR polarization curve. Our studies on the electrocatalytic activity of **3** for OR are continuing with the aim of identifying the reaction steps involved in the OR mechanism, decreasing overvoltage and increasing stability, using various types of modified electrodes, and will be presented in a further report, with the relevant kinetic investigation, in detail. At this stage, it should be noted that the total number of electrons transferred was found to vary from 3.26 (37% H_2O_2 and 63% H_2O) in lower overpotential regions to 3.84 (8% H_2O_2 and 92% H_2O) in higher overpotential region, by using a rotating ring–disk voltammetry technique. The detection of H_2O in greater amounts than H_2O_2 at all potentials of the polarization curve suggested that OR occurs through both a 4-electron mechanism to produce H_2O and a 2-electron mechanism to give H_2O_2. It is also possible to propose that OR occurs *via* a four-electron mechanism, but can not go to completion in some catalytic sites and produce H_2O_2.

Mononuclear Co(II) Pcs are known to catalyze OR, usually to form only H_2O_2 *via* a 2-electron process.[14] The encouraging catalytic activity of **3** has vital importance for OR in polymer electrolyte membrane (PEM) fuel cell applications. It can be attributed to the enhanced interaction between two redox-active metal centers due to the face-to-face structure that promotes O–O bond breakage and probably causes an easier reduction to H_2O, as compared to mononuclear Pcs. This type of enhanced catalytic activity towards OR was suggested by the groups of Collman and Chang for various covalently linked porphyrin dimers.[11] They concluded that some flexible porphyrin dimers such as anthracene pillar dicobalt porphyrin and dicobalt porphyrins linked by two amide chains are capable of reducing oxygen to water mainly *via* the 4-electron pathway without the intermediacy of H_2O_2, while rigid systems with inappropriate center-to-center distances precluded any concerted coordination of the O_2 molecule to the cobalt located in the center of the porphyrin cores, and thus did not show high catalytic performance in comparison with the former.[15] On the other hand, Bruice *et al.* reported that the aza bridged closely interspaced cofacial porphyrine dimers can also catalyze effectively the 4-electron reduction of O_2 to water.[12] They also stated that the precise geometry of the biscobalt tetraphenylporphyrin dimer is the crucial factor that determines $2e^-$ *versus* $4e^-$ reduction of O_2 while the reduction potential is independent of the path. The onset potential of OR where the current starts to increase is around 0.55 V *vs.* SCE in this study. It appears at a more positive potential, compared to those reported by Bruice *et al.* for some similar complexes,[12] suggesting that CoPc (**3**) catalyzes OR effectively to produce water as the main product and also some H_2O_2.

The catalytic activity of metallophthalocyanines are generally attributed to their subsequent one-electron reduction and oxidation abilities in a broad potential range. Macrocyclic metal centers also have a remarkable influence on catalytic performance. In the case of a redox-active metal center, the interaction between the metal center and the O_2 molecules is enhanced as a result of the partial electron transfer from the filled d orbitals of the metal to the empty or partially filled π^* orbitals of oxygen. The high catalytic activity of **3**, as compared to **4**, can be attributed to its ability to bind dioxygen due to its distinctive coordinating properties.

The temperature dependence of the direct current conductivity of **3** and **4** in their films was examined during heating processes. By analyzing the dc electrical behaviour of the films, it was found that the experimental data are described by a thermally activated conductivity dependence on temperature with an activation energy of 0.60 and 0.85 eV for the compounds **3** and **4**, respectively. Well defined straight lines in the Arrhenius plots (logarithms of dc conductivity *versus* inverse temperature) suggest the presence of only one conduction mechanism, assuming that the dominant levels are the conduction and valence bands over the whole temperature range for the films of **3** and **4**. The observed electrical conductivity values at room temperature for **3** and **4** are 2.1×10^{-10} and 6.2×10^{-11} S cm^{-1}, respectively.

The frequency dependence of the ac conductivity, $\sigma_{ac}(\omega)$, for different temperature values between 300 and 440 K was also investigated for the samples. The frequency dependence of the ac conductivity is shown in Fig. 5 for both compounds as a plot of ln σ_{ac} *versus* ln ω at 300 K and 380 K. It can be seen from this figure that the ac conductivity increases with frequency for all temperatures. The general observed frequency dependence of the ac conductivity in disordered systems, such as phthalocyanine, is that the ac conductivity obeys an empirical power law of the form $\sigma_{ac} = A\omega^s$, where ω is the angular frequency, A and the frequency exponent, s, are material dependent constants.

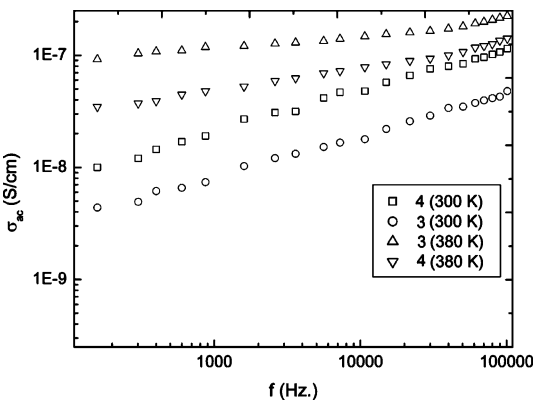

Fig. 5 Frequency dependent conductivity, σ_{ac}, at different temperatures.

In order to explain the behaviour of ac conductivity with both temperature and frequency, different theoretical models have been proposed to correlate the conduction mechanism of ac conductivity with the temperature dependence of frequency exponent s. One of these models assumes that carrier motion occurs through

quantum mechanical tunelling (QMT) between localized states near the Fermi level. For the QMT model, frequency exponent s is temperature independent but frequency dependent. In the second model, which is known as the correlated barrier hopping (CBH) model, the electrons in charged defect states hop over the coulomb barrier. In these two models, the frequency exponent s is found to have two different trends with temperature and frequency.[16] According to the QMT model, frequency exponent s is temperature independent but frequency dependent. On the other hand, the CBH model predicts a temperature dependent s which is given by

$$s = 1 - 6kT/W_m$$

where W_m is the binding energy, which is defined as the energy required to remove an electron completely from one site to the other site, and k is Boltzmann's constant. The values of the frequency exponent s were calculated from the slope of the measured ln σ_{ac} *versus* ln ω graphs. Our calculations showed that s is definitely a function of temperature for both compounds and shows a general tendency to decrease with increasing temperature. This is in agreement with the prediction of the CBH model.

It is well known that the adsorption of the gas molecules on the surface of a Pc film plays an important role in the change in physical or chemical properties of these materials. The effect of the various concentrations of SO_2, CO_2, CO and VOC (volatile organic chemical) vapors on the conductivity of the **3** and **4** were tested at different temperatures. It was found that compound **3** is not sensitive for the gases investigated, with the exception of SO_2 for which very high sensitivity was obtained. The response characteristics of **3** to the various concentrations (50–250 ppm) of SO_2 at room temperature are shown in Fig 6. During the measurements, the film was exposed to SO_2 repeatedly. Each cycle of exposure lasted for 5 min, followed by recovery in dry nitrogen for another 5 min. It was observed that the current increased sharply in the initial doping stage for a few minutes and the rate of increase slowed down. Although a complete steady-state current cannot be approached during a period of 5 min, the increase in current is adequate to indicate the presence of SO_2 gas in the atmosphere. After exposure to SO_2 gas for several minutes, purging with dry nitrogen leads to an initial fast decrease followed by a slow drift and the current reaches its initial value after the SO_2 gas is turned off. This proves that the adsorption process is reversible. The response characteristics of the film can be explained as follows. The adsorption of SO_2 molecules on the film surface leads to the creation of an acceptor level near the surface. These acceptor states, which lie below the Fermi level at the initial stage of adsorption, make the trapping of valance electrons easy. When the sensor is then exposed to dry nitrogen, desorption of adsorbed SO_2 molecules from the surface of the active sensing layer occurs. This decreases the acceptor concentration and thus the current.

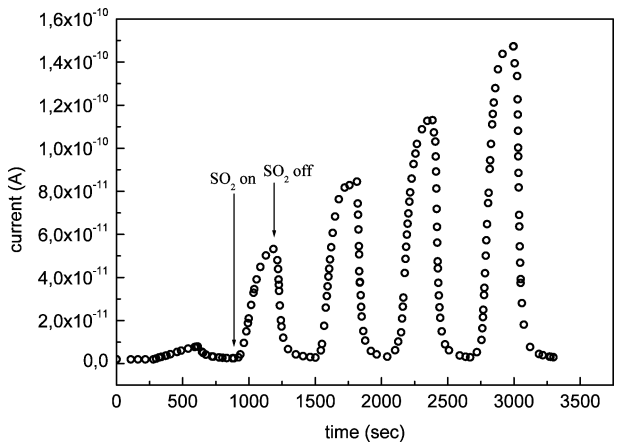

Fig. 6 Response characteristics of the **3** coated sensor to 50, 100, 150, 200 and 250 ppm of SO_2 gas at room temperature.

3. Experimental

3.1 Synthesis of compounds 3 and 4

The suspension of each BTMPc (0.142 g, 0.085 mmol for **1** and 0.127 g, 0.075 mmol for **2**) and NaH (0.016 g, 0.68 mmol for **1** and 0.014 g, 0.60 mmol for **2**) in DMF (30 ml) was stirred at 100 °C for 2 h under N_2. The reaction mixture was allowed to cool at room temperature, and HDFID (0.390 g, 0.68 mmol or 0.344 g, 0.60 mmol) was added portionwise to the mixture with stirring. The reaction mixture was kept at 120 °C for an additional 6 h with stirring under N_2. To the cooled reaction mixture, 50 ml of ethanol were added and the precipitate was filtered off. The crude product was dried *in vacuo*. Compound **3** was isolated using a silica gel packed column using a gradient of THF–DMF [(2.0 : 0.1–2.0 : 1.0) (v/v)] as eluent. In the case of **4**, the complex was dissolved in DMF by heating and successively precipitating in boiling acetic acid, water, methanol and acetone, and dried *in vacuo*. These compounds are soluble in DMF and DMSO and insoluble in MeOH, EtOH, and THF.

BTMPcs(Co) (3). Yield: 0.292 g, 65%. Mp > 300 °C. UV-vis (DMF) λ, nm (log ε): 671 (4.42), 625 (4.25), 331 (4.45). IR (KBr pellet) ν, cm^{-1}: 3061 (arom-CH), 2937–2880 (aliph-CH), 1767–1713 (C=N), 1605 (Ar-C=C), 1466, 1260 (aliph-O-Ar), 1230–1120 (C–F). MS (MALDI-TOF), m/z: 5243 $[M + H]^+$. Anal. calcd for $C_{164}H_{92}N_{16}F_{136}O_{16}Co_2$: C, 37.56; H, 1.77; N, 4.27%. Found: C, 37.42; H, 1.73; N, 4.18%.

BTMPc(Cu) (4). Yield: 0.243 g, 61%. Mp > 300 °C. UV-vis (DMF) λ, nm (log ε): 687 (4.77), 645 (4.38), 357 (4.55). IR (KBr pellet) ν, cm^{-1}: 3061 (arom-CH), 2925–2853 (aliph-CH), 1766–1707 (C=N), 1601 (Ar-C=C), 1463, 1261 (aliph-O-Ar), 1226–1116 (C–F). MS (MALDI-TOF), m/z: 5251 $[M + H]^+$. Anal. calcd for $C_{164}H_{92}N_{16}F_{136}O_{16}Cu_2$: C, 38.04; H, 1.77; N, 4.27%. Found: C, 37.93; H, 1.75; N, 4.31%.

3.2 MALDI sample preparation

Supramolecular complex **3** was prepared at a concentration of 4 mg mL^{-1} in dimethylformamide for MALDI-MS analysis. 2,5-DHB was chosen as the best MALDI matrix and prepared in acetonitrile at a concentration of 20 mg mL^{-1}. MALDI samples were prepared by mixing the solutions (1 : 10 v/v) in a 0.5 mL Eppendorf® micro tube. Finally 1 μL of this mixture was deposited on the sample plate, dried at room temperature and then analyzed.

MALDI samples for **4** were prepared by mixing the complex solution (5 mg mL^{-1} in dimethylformaide) with the matrix solution [CHCA (20 mg mL^{-1} in tetrahyrofuran with 0.5% trifluoroaceti-cacid)] (1 : 10 v/v) in a 0.5 mL Eppendorf® micro tube. Finally

1 μL of this mixture was deposited on the sample plate, dried at room temperature and then analyzed.

3.3 MALDI mass spectrometry

Mass spectra were acquired on a Voyager-DE™ PRO MALDI-TOF mass spectrometer (Applied Biosystems, USA) equipped with a nitrogen UV-laser ($\lambda = 337$ nm) at 10^{-8} Torr using delayed extraction mode (delay 375 ns) by changing the laser intensity, if necessary. Acceleration potential was 25 kV for the spectra recorded in linear mode and all spectra were the average of 50 shots. Then, data were transferred to a personal computer for further processing.

3.4 Electrochemical and electrocatalytic measurements

The electrochemical measurements were carried out using a Gamry Reference 600 potentiostat. The procedure for the electrochemical measurements of the complexes in non-aqueous solution is described in detail elsewhere.[9] The electrocatalytic measurements were performed on the rotating disc electrode with a glassy carbon disc (5 mm dia.) in O_2 saturated 0.5 M H_2SO_4 aqueous solution at a 0.005 V s^{-1} sweep rate at 298 K, using a Pine Instrument Company AFMSRX modulator speed rotator. The counter electrode was a Pt spiral and the reference electrode was a saturated calomel electrode (SCE). In order to disperse the catalysts on a carbon support, a mixture of the Pc complex, Vulcan XC-72 (Cabot Co.) and 5% wt Nafion® solution (Aldrich) in absolute ethanol was prepared and ultrasonically homogenized for half an hour. A given volume of this ink was deposited using a micropipette onto a freshly polished GCE leading to a catalyst loading of 125 μg cm^{-2}. In order to obtain a total coverage of the glassy carbon surface, the deposited drop of ink was dried with pulsed air at ambient temperature to evaporate the solvent quickly. Each voltammogram was recorded with a freshly prepared electrode.

3.5 Electrical and gas sensing measurements

The measurement electrodes used in the conductivity and gas sensing measurements consist of an interdigital array of metal electrodes photolithographically patterned on a pre-cleaned glass substrate. Glass substrates were throughly cleaned ultrasonically and then coated with 100 Å of chromium followed by 1200 Å of gold in an Edwards Auto 500 coater system. The film was patterned photolithographically and etched to provide 10 finger pairs of electrodes having a width of 100 μm, spaced 100 μm from the adjacent electrodes. Gold was selected as the electrode material, since it is well-known that it forms ohmic contact to phthalocyanine. Thin films of the compounds were prepared by the spin coating method on ohmic gold interdigital electrodes (IDT). For the spin coating, coating solutions were prepared by dissolving the Pcs in extra pure grade DMF at concentrations of 5×10^{-2} M for both compounds. 20 μL of such solutions were added with a glass pipette onto the IDT structure held on the spinner (Speciality Coatings Systems Inc., Model P6700 Series). The substrate was spun at 2000 rpm for 30 s and the solvent had evaporated during this period, producing a homogeneous film of phthalocyanine derivatives. The substrate temperature was kept constant at 300 K during deposition of the materials over the electrodes. dc Conductivity measurements were performed between 300 K and 440 K by using a Keithley 617 electrometer. ac Conductivity measurements were carried out with a Keithley 3330 LCZ meter in the frequency range 40–10^5 Hz, and in the temperature range from 300 K to 440 K. All the measurements were performed under 10^{-3} mbar of gas in the dark. The effect of the SO_2, CO_2, CO and VOC vapors on the conductivity of the films was measured in a homemade Teflon chamber implemented in our laboratory where dry nitrogen was used as carrier gas. After each MPc sensor in the chamber was stable, it was exposed to five different concentrations of the target gases. The test gas were mixed with dry nitrogen (N_2) using computer driven mass flow controllers (MKS Inst.). A typical experiment consisted of exposure to test gases and subsequent purging with dry nitrogen. Both conductivity and gas sensing data were recorded using an IEEE 488 data acquisition system incorporated into a personnel computer.

Conclusions

In conclusion, the novel cofacial or BTMPc derivatives bearing eight heptadecafluorodecyl groups (**3** and **4**) were obtained from the precursor cofacial dimers of BTMPcs (**1** and **2**) accommodating eight hydroxy groups and heptadecafluoro-10-iododecane (HDFID), and characterized by spectroscopic methods. Ball-type Co_2Pc_2 complex **3** displayed high catalytic activity for OR as compared with the ball-type Cu_2Pc_2 complex. The high catalytic activity of **3** can be attributed to the rigid cofacial structure involving two redox-active metal centers. This is very important for the OR in PEM fuel cell applications. Both dc and ac conduction mechanisms as a function of temperature were investigated. Whilst the dc behavior of the films is described by a thermally activated conductivity dependence on temperature, the ac conduction mechanism is explained by the CBH model. The sensitivity of the films to SO_2, CO_2, CO and VOC vapors was also studied and very high sensitivity to low concentrations of SO_2 gas were obtained using compound **3**.

Acknowledgements

We thank The Turkish Academy of Sciences (TUBA), Marmara University and The Scientific and Technological Research Council of Turkey (TUBITAK) (Project Nos: 108T272, 107T834 and, 106T326) for their support.

Notes and references

1 A. Y. Tolbin, A. V. Ivanov, L. G. Tamilova and N. S. Zefirov, *Mendeleev Commun.*, 2002, 96.
2 T. Ceyhan, A. Altındal, A. R. Özkaya, M. K. Erbil, B. Salih and Ö. Bekaroğlu, *Chem. Commun.*, 2006, 320.
3 Z. Odabaş, A. Altındal, A. R. Özkaya, M. Bulut, B. Salih and Ö. Bekaroğlu, *Polyhedron*, 2007, **26**, 695.
4 M. Özer, A. Altındal, A. R. Özkaya, B. Salih, M. Bulut and Ö. Bekaroğlu, *Eur. J. Inorg. Chem.*, 2007, 3519.
5 M. Özer, A. Altındal, B. Salih, M. Bulut and Ö. Bekaroğlu, *Tetrahedron Lett.*, 2008, **49**, 896.
6 Z. Odabaş, A. Altındal, A. R. Özkaya, M. Bulut, B. Salih and Ö. Bekaroğlu, *Polyhedron*, 2007, **26**, 3505.
7 Z. Odabaş, A. Altındal, B. Salih, M. Bulut and Ö. Bekaroğlu, *Tetrahedron Lett.*, 2007, **48**, 6326.

8 M. Canlıca, A. Altındal, A. R. Özkaya, B. Salih and Ö. Bekaroğlu, *Polyhedron*, 2008, **27**, 1883.
9 S. Altun, A. Altındal, A. R. Özkaya, M. Bulut and Ö. Bekaroğlu, *Tetrahedron Lett.*, 2008, **49**, 4483.
10 S. P. Keizer, J. Mack, B. A. Bench, S. M. Gorun and M. J. Stillman, *J. Am. Chem. Soc.*, 2003, **125**, 7067.
11 (*a*) J. P. Collman, M. Marrocco, P. Denisevich, C. Koval and F. C. Anson, *J. Electroanal. Chem. Interfacial Electrochem.*, 1979, **101**, 117; (*b*) J. P. Collman, P. Denisevich, Y. Konai, M. Marrocco, C. Koval and F. C. Anson, *J. Am. Chem. Soc.*, 1980, **102**, 6027; (*c*) J. P. Collman, N. H. Hendricks, C. R. Leidner, E. Ngameni and M. L'Her, *Inorg. Chem.*, 1988, **27**, 387; (*d*) R. R. Duran, C. S. Bencosme, J. P. Collman and F. C. Anson, *J. Am. Chem. Soc.*, 1983, **105**, 2710; (*e*) H. Y. Liu, I. Abdalmuhdi, C. K. Chang and F. C. Anson, *J. Phys. Chem.*, 1985, **89**, 665; (*f*) H. Y. Liu, M. J. Weaver, C. B. Wang and C. K. Chang, *J. Electroanal. Chem. Interfacial Electrochem.*, 1983, **145**, 439; (*g*) C. K. Chang, H. Y. Liu and I. Abdalmuhdi, *J. Am. Chem. Soc.*, 1984, **106**, 2725.
12 R. Karaman, S. Jeon, Ö. Almarsson and T. C. Bruice, *J. Am. Chem. Soc.*, 1992, **114**, 4899.
13 S. Baronton, C. Coutanceau, C. Roux, F. Hahn and J.-M. Leger, *J. Electroanal. Chem.*, 2005, **577**, 223.
14 L. Zhang, J. Zhang, D. P. Wilkinson and H. Wang, *J. Power Sources*, 2006, **15**, 171.
15 J. P. Collman, F. C. Anson, S. Bencosme, A. Chong, T. Collins, P. Denisevich , E. Evitt, T. Geiger, J. A. Ibers, G. Lameson, Y. Konai, C. Koval, K. Meier, P. Okaley, R. Pettman, E. Schmittou and J. Sessler, in *Organic Synthesis Today and Tomorrow*, ed. B. M. Trost and C. R. Hutchinson, Pergamon Press, Oxford, 1981, pp. 29–45.
16 S. R. Elliot, *Adv. Phys.*, 1987, **2**, 135.